

3D-Properties: Identifying Challenges in DPO and Charting a Path Forward

Yuzi Yan^{1,3‡}, Yibo Miao^{2,3‡}, Jialian Li³, Yipin Zhang³, Jian Xie³, Zhijie Deng^{2*}, Dong Yan^{3*}

¹Department of Electronic Engineering, Tsinghua University

²Qing Yuan Research Institute, SEIEE, Shanghai Jiao Tong University

³Baichuan AI

yan-yz17@tsinghua.org.cn, {miaoyibo, zhijied}@sjtu.edu.cn,
lijialian7@163.com, zypzyp665@gmail.com, xiejian1990@gmail.com, sproblvem@gmail.com

Abstract

Aligning large language models (LLMs) with human preference has recently gained tremendous attention, with the canonical yet costly RLHF-PPO and the simple and straightforward Direct Preference Optimization (DPO) as two examples. Despite the efficiency, DPO has rarely been used in the state-of-the-art production-level LLMs, implying its potential pathologies. In this work, we revisit DPO with a comprehensive examination of its empirical efficacy and a systematic comparison with RLHF-PPO. We identify the **3D**-properties of DPO’s learning outcomes: the **D**rastring drop in the likelihood of rejected responses, the **D**egradation into LLM unlearning, and the **D**ispersion effect on unseen responses through experiments with both a carefully designed toy model and practical LLMs on tasks including mathematical problem-solving and instruction following. These findings inherently connect to some observations made by related works and we additionally contribute a plausible theoretical explanation for them. Accordingly, we propose easy regularization methods to mitigate the issues caused by **3D**-properties, improving the training stability and final performance of DPO. Our contributions also include an investigation into how the distribution of the paired preference data impacts the effectiveness of DPO. We hope this work could offer research directions to narrow the gap between reward-free preference learning methods and reward-based ones.

1 Introduction

Large language models (LLMs) trained on extensive datasets have shown outstanding performance across diverse tasks and domains [28, 10, 16, 35]. Various techniques for fine-tuning LLMs have been developed, including the well-known Supervised Fine-Tuning (SFT) and Reinforcement Learning from Human Feedback (RLHF) [1, 28]. SFT focuses on tailoring the LLMs’ responses for specific tasks directly with labeled data, whereas RLHF improves LLMs through feedback data reflecting human preferences. In particular, RLHF is pushing the application boundaries of both closed-source [20, 3, 27] and open-source LLMs [28, 33], due to the necessity for polishing the value, fairness, and helpfulness of LLMs in practical scenarios [38, 25, 21].

Existing RLHF methods can be majorly categorized into two classes based on whether the reward signal is explicitly modeled. *Reward-based alignment* pioneered by OpenAI [21, 1, 28] first trains a reward model from user preferences, typically through Maximum Likelihood Estimation (MLE),

[‡]Equal contribution.

[†]Interns at Baichuan

*Corresponding authors.

and then leverages actor-critic algorithms such as Proximal Policy Optimization (PPO) [24] to tune the SFT model to realize alignment. This approach often requires substantial computational resources and suffers from sample inefficiency [9]. Conversely, another class of methods, known as *reward-free alignment*, such as Direct Preference Optimization (DPO) [23], Identity Preference Optimization (IPO) [4], and Sequence Likelihood Calibration (SLiC) [36], do not rely on an extra reward model. These approaches offer a more resource-efficient alternative by optimizing the policy directly from preferences, therefore attracting much attention from the academic society. In this work, we commence our analysis with the vanilla DP as a case study, subsequently extending our findings to encompass broader reward-free alignment strategies.

Despite the simplicity and promise of DPO, a variety of phenomena that cannot be clearly understood or explained have been observed and reported in practice. A representative counter-intuitive observation is that the likelihood of both the chosen (i.e., preferred) and the rejected (i.e., less preferred) response will decrease over DPO’s training process [34, 19], while the likelihood of some tokens deviating from the dataset increases [31]. More observations are summarized in Section 2.1. Arguably, purely empirical investigation on applying or improving DPO without a deep exploration and understanding of these phenomena would suffer from low efficiency.

In this paper, we delve into the issues surrounding DPO and its variants from both theoretical and practical perspectives. Our investigation identifies inherent instability in the DPO training process, which we summarize as the **3D**-properties: **D**rastic drop in the likelihood of rejected responses, **D**egradation into LLM unlearning, and the **D**ispersion effect on unseen responses. Our analytical framework comprehensively elucidates the reasons behind these phenomena, demonstrating that the **3D**-properties significantly undermine DPO’s performance. Moreover, we demonstrate that several DPO variants, such as IPO and SLiC, inherently address these challenges, hence enjoying enhanced performance. Furthermore, our findings confirm that the data distribution of the preference dataset critically influences DPO’s effectiveness. Notably, on-policy DPO exhibits the best performance, which aligns perfectly with recent empirical studies [26, 13].

We propose several regularization methods to enhance the stability of DPO, including adjusting positive and negative weights adaptively and incorporating SFT loss. Our results indicate a potential fundamental trade-off within the DPO algorithm: balancing the mitigation of the 3D-properties against preserving model generalization in preference learning. Furthermore, we thoroughly compare DPO with the state-of-the-art reward-based method RLHF-PPO, revealing that the latter’s superiority may in part stem from its avoidance of 3D-properties. Our experimental approach begins with the design of a toy model to quickly validate our hypotheses, followed by a rigorous test of the actual performance of Baichuan2-13B and Baichuan2-33B [33] on tasks such as mathematical problem solving and instruction following.

2 Preliminaries

Large Language Model (LLM). An LLM defines a θ -parameterized conditional distribution $\pi_\theta(a|x)$, which takes a prompt x as input and produces a response a . More specifically, the sampling from LLMs is performed in an auto-regressive manner:

$$\pi_\theta(a|x) = \prod_t \pi_\theta(a_t|x, a_{1:t-1}), \quad (1)$$

where a_t is the t -th token in the response a and $a_{1:t-1}$ are tokens in the response before a_t .

RLHF-PPO. Training LLMs typically involves three stages: Pretraining, SFT, and RLHF. In this section, we outline the standard RLHF-PPO paradigm, widely adopted in advanced research [38, 21].

Beginning with a well-trained SFT model, denoted as π_0 , we proceed by sampling two responses from π_0 for each instance in a given prompt set. Subsequently, we compile a set of comparisons $\mathcal{D} = \{(x, a^+, a^-)\}$, where a^+ and a^- denote human-preferred and human-dispreferred completions, respectively. The distribution of the preference dataset is assumed to follow the Bradley-Terry model [7], i.e., the probability of response a^+ is better than a^- is given by:

$$p_r(a^+ \succ a^-|x) = \frac{\exp(r(x, a^+))}{\exp(r(x, a^+)) + \exp(r(x, a^-))} = \sigma(r(x, a^+) - r(x, a^-)), \quad (2)$$

where \succ represents the preference relation, and $\sigma(x) = \frac{1}{1+e^{-x}}$ is the sigmoid function. To train a reward model r , we maximize the log-likelihood of the observed preferences by minimizing the following loss function:

$$\ell_R(r) = - \sum_{(x, a^+, a^-)} \log p_r(a^+ \succ a^- | x) = - \sum_{(x, a^+, a^-)} \log \sigma(r(x, a^+) - r(x, a^-)). \quad (3)$$

During the RL optimization phase, we update the LM to maximize the return from the learned reward model using the following principle:

$$\max_{\theta} J_r(\theta) = \max_{\theta} \sum_x \mathbb{E}_{a \sim \pi_{\theta}(\cdot | x)} \left[r(x, a) - \beta \log \frac{\pi_{\theta}(a | x)}{\pi_0(a | x)} \right], \quad (4)$$

where π_{θ} is initialized as π_0 and β controls the deviation from the original model. PPO [24] is typically used to solve the problem in practice. Algorithms that optimize the policy using a separate reward model are referred to as *reward-based* alignment.

DPO. Instead of learning a separate reward model, DPO [23] directly optimizes the policy π_{θ} over preference data. DPO leverages a particular choice of reward model parameterization that enables the extraction of its optimal policy in closed form, without an RL training loop:

$$\ell_{\text{DPO}}(\theta) = - \sum_{(x, a^+, a^-)} \log \sigma \left[\beta \log \frac{\pi_{\theta}(a^+ | x)}{\pi_0(a^+ | x)} - \beta \log \frac{\pi_{\theta}(a^- | x)}{\pi_0(a^- | x)} \right]. \quad (5)$$

As shown, DPO leverages logistic regression loss to directly fine-tune the LM on preference data. This approach, along with its various variants [36, 2, 4], is referred to as *reward-free* alignment due to the elimination of an explicit reward model.

2.1 Underexplored Facts about the DPO Algorithm

Though the absence of the need for additional reward model training makes DPO particularly attractive, there are still many underexplored observations. The most concerning issue is, to the best of our knowledge, few models using DPO (or other reward-free algorithm) have achieved performance comparable to the state-of-the-art closed-source LLMs such as OpenAI’s ChatGPT or Anthropic’s Claude, which reportedly use PPO methods during training. Besides, many other phenomena have been reported but lack comprehensive theoretical explanations. Here we make a summary for clarity.

Fact 1. During the vanilla DPO training, the likelihood of both the chosen and rejected responses in the preference datasets tends to decrease [19], whereas the likelihood of unseen tokens not appearing in the preference pairs tends to increase [31].

Fact 2. Compared with RLHF-PPO, the performance of DPO is relatively unstable and sub-optimal [31].

Fact 3. The performance of DPO is significantly affected by the distribution shift between the model outputs and the preference dataset. In general, on-policy DPO, where both the chosen responses and the rejected response are sampled from the policy model π_{θ} , outperforms other variants [26].

In the following section, we will offer theoretical explanations for these facts.

3 The Fundamental Limitation of Vanilla DPO: 3D-Properties

We first identify a critical flaw inherent in the vanilla DPO framework. At first glance, the loss function of standard DPO, as defined in Equation 5, seems to be divided into two segments. The term $\log \frac{\pi_{\theta}(a^+ | x)}{\pi_0(a^+ | x)}$ aims to increase the likelihood of the chosen response, whereas the term $\log \frac{\pi_{\theta}(a^- | x)}{\pi_0(a^- | x)}$ seeks to reduce the likelihood of the rejected response. Yet, this straightforward interpretation can lead to a serious overlook of core issues, which we define through the 3D-properties of vanilla DPO:

Property 1 (Drastic drop in rejected response likelihood). The likelihood of a rejected response changes much more rapidly than that of a chosen response.

Property 2 (Degradation into LLM unlearning). DPO will gradually fail to control the optimization direction of chosen responses and degrade into solely unlearning the rejected responses as the optimization progresses.

Property 3 (Dispersion effect on unseen responses). As the training of DPO progresses, the likelihood associated with both chosen and rejected responses will gradually decrease. Concurrently, the likelihood of generating responses not present in the dataset will increase.

In the forthcoming sections, we first provide the theoretical foundations, followed by detailed explanations of the observations discussed in Section 2.1. Subsequently, we introduce a simplified toy model specifically designed to facilitate synthetic experiments, thereby enhancing the persuasiveness of our arguments.

3.1 Theoretical Foundation

The loss function for DPO (Equation 5) can be re-written by:

$$\ell^{\text{DPO}}(\theta) = \sum_{(x, a^+, a^-)} \log \left(1 + \left(\frac{\pi_0(a^+|x)}{\pi_0(a^-|x)} \frac{\pi_\theta(a^-|x)}{\pi_\theta(a^+|x)} \right)^\beta \right). \quad (6)$$

For a given triple (x, a^+, a^-) , let

$$\alpha := \left(\frac{\pi_0(a^+|x)}{\pi_0(a^-|x)} \right)^\beta, \quad \pi^+ := \pi(a^+|x), \quad \pi^- := \pi(a^-|x), \quad z = \frac{\pi_\theta(a^-|x)}{\pi_\theta(a^+|x)}.$$

Then we have

$$\begin{aligned} \frac{\partial \ell^{\text{DPO}}}{\partial \pi^+} &= \frac{\partial \log(1 + \alpha z^\beta)}{\partial z} \frac{\partial z}{\partial \pi^+} = \frac{\alpha \beta}{1 + \alpha z^\beta} z^{\beta-1} \frac{\partial z}{\partial \pi^+}, \\ \frac{\partial \ell^{\text{DPO}}}{\partial \pi^-} &= \frac{\partial \log(1 + \alpha z^\beta)}{\partial z} \frac{\partial z}{\partial \pi^-} = \frac{\alpha \beta}{1 + \alpha z^\beta} z^{\beta-1} \frac{\partial z}{\partial \pi^-}. \end{aligned}$$

We have the following observations:

Corollary 1 (Explanation for Property 1). The gradient ratio is:

$$\frac{\partial \ell^{\text{DPO}}}{\partial \pi^-} / \frac{\partial \ell^{\text{DPO}}}{\partial \pi^+} = \frac{\partial z}{\partial \pi^-} / \frac{\partial z}{\partial \pi^+} = \frac{\pi^+}{\pi^-}.$$

From the above corollary, we can observe that the gradient with respect to $\partial \pi^-$ not only tends to increase but also accelerates in growth as the pair (π^+, π^-) is optimized toward $(1, 0)$.

Corollary 2 (Explanation for Property 2). As $\pi^- \rightarrow 0$ and given that $\beta < 1$, $\frac{\partial \ell^{\text{DPO}}}{\partial \pi^+}$, which is proportional to $(\pi^-)^\beta$, tends towards zero. Conversely, $\frac{\partial \ell^{\text{DPO}}}{\partial \pi^-}$, proportional to $(\pi^-)^{\beta-1}$, approaches infinity. In this case, the gradient associated with the rejected response becomes exceedingly large, while the gradient for the chosen response diminishes significantly. This dynamic leads to a situation where DPO progressively focuses on unlearning the rejected responses.

Corollary 3 (Explanation for Property 3). When π^- drastically drops to 0, the gradient on π^+ gradually fails and the likelihood of the chosen response is likely to decrease randomly. As both π^+ and π^- decrease, the generation probability will randomly disperse into other unseen responses out of the preference dataset.

Based on these theoretical insights, we can further explore the observed facts in Section 2.1. Fact 1 can be explained directly. For Fact 2, we will show that 3D-properties don't exist in the RLHF-PPO framework in Section 4. For Fact 3, we will demonstrate that the distribution gap between the model's output and the preference dataset dictates the strength of influence exerted by the 3D-properties. Comparatively, the impact of 3D-properties is less pronounced in on-policy DPO.

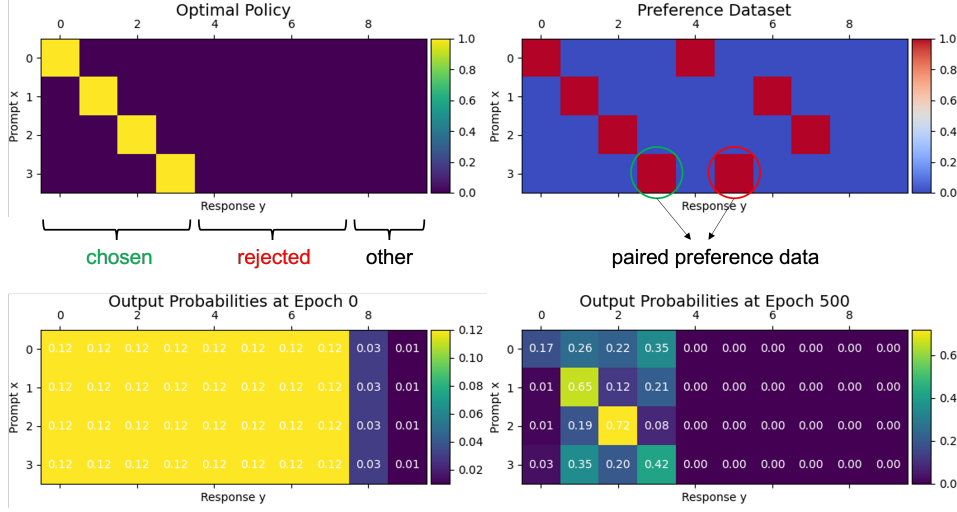


Figure 1: Toy model setup, preference dataset construction, and results before and after DPO training.

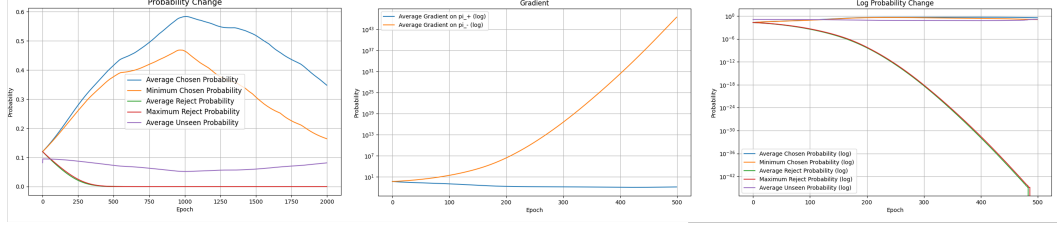


Figure 2: Vanilla DPO performance on toy model.

3.2 Synthetic Validation in a Toy Model

Before conducting experiments on real LLMs, we introduce a light toy model, which can help us validate Corollary 1 to 3 in a straightforward way.

3.2.1 Toy Model Setup

We construct discrete spaces consisting of 4 prompts and 10 responses. The policy π_θ is implemented as a three-layer MLP that processes a one-hot vector to produce a categorical distribution over the responses. The first 4 dimensions of the response space correspond to the chosen responses, dimensions 5 through 8 to the rejected responses, and the final 2 dimensions to unseen responses not present in the preference dataset. We configure the optimal response to correspond directly with its respective prompt; for example, response 1 is optimal for prompt 1. This setup is illustrated in Figure 1.

Step 1. We simulate the Pretraining/SFT process by manually specifying the output probabilities and using them as labels to train the model.

Step 2. We construct the preference dataset and simulate the DPO process. The dataset is constructed using optimally chosen responses and randomly selected rejected responses to form paired data.

3.2.2 Results

Initially, we set the likelihood of each chosen and rejected response at 0.12, allowing us to treat both as on-policy. The results are shown in Figure 2. During the early phases of DPO, the likelihood of chosen responses increases, while that of rejected responses decreases. However, as training progresses and $\pi_\theta(a^-|x)$ approaches zero (illustrated in the third figure), the likelihood of chosen responses begins to diminish. Concurrently, in the second figure, we have plotted the changes in gradient, which shows that the absolute value of $\partial \ell^{\text{DPO}} / \partial \pi^-$ increases sharply. In the degradation

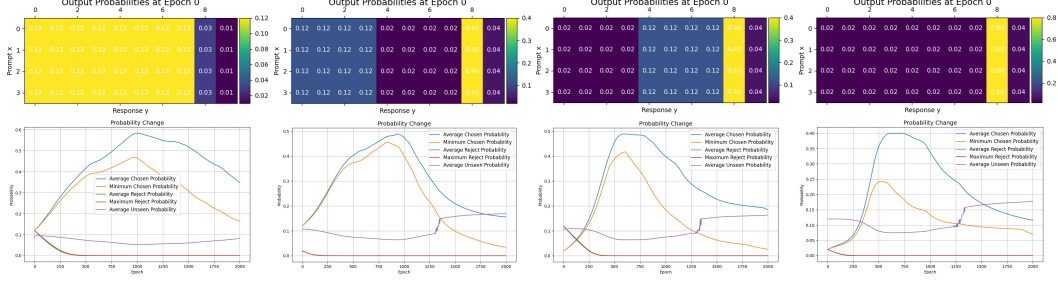


Figure 3: From left to right, the figures present the initial state and the changing process of the likelihood of each response for Scenario 1 to Scenario 4. Scenario 1: chosen on-policy and rejected on-policy. Scenario 2: chosen off-policy and rejected on-policy. Scenario 3: chosen on-policy and rejected off-policy. Scenario 4: chosen off-policy and rejected off-policy.

phase, with both chosen and rejected responses decreasing in likelihood, the probability is reassigned to unseen responses. These findings are consistent with our previous theoretical analysis.

We now understand that the rate at which $\pi_\theta(a^-|x)$ declines is a critical factor in determining the severity of the 3D-properties’ impact. This leads us to propose the following:

Proposition 1. To lessen the severity of the 3D-properties, it is advantageous to moderate the rate at which the likelihood of rejected responses declines.

Furthermore, this insight helps explain why on-policy DPO is generally more effective (Fact.3). Compared to off-policy DPO, on-policy DPO starts with a higher likelihood of rejected responses, thereby prolonging the time it takes for their likelihood to diminish. On the other hand, the higher initial probability within the training set also minimizes the dispersion effect on unseen tokens.

To empirically validate these differences between on-policy and off-policy DPO, we conducted experiments using our toy model. We configure four scenarios by adjusting the initial distribution of the outputs in **Step 1**. The initial state and subsequent changes in the likelihood of each response are depicted in Figure 3. Notably, the 3D-properties in Scenario 1, where both chosen responses and rejected responses are on-policy, are relatively mild, as evidenced by both the high peak probability of the optimal response (approximately 0.6) and the minimal dispersion effect on unseen responses. Further detailed results and analyses of these four scenarios are provided in Appendix D.

3.3 Regularization Techniques

Inspired by Proposition 1, we introduce two straightforward regularization techniques. The first technique employs variable values of β to control the rate at which the likelihood of rejected responses declines. The second technique involves augmenting the DPO loss with an SFT loss, a strategy that has been shown to significantly enhance the stability of DPO in previous studies, such as those documented in [15, 32]. These regularization methods have shown promising results in our toy model. Detailed discussions and experimental outcomes are presented in Appendix B.2.

4 Non-existence of 3D-properties in RLHF-PPO

In this section, we show that 3D-properties do not manifest in the commonly used alignment methods RLHF-PPO, which may account for why DPO methods only achieve sub-optimal performance in comparison.

In the RLHF-PPO algorithm described in [21], the process is twofold: first, training a reward model (RM), followed by optimization using a reinforcement learning algorithm such as PPO. The loss function for the RM is defined as:

$$\ell^{\text{RM}}(\theta) = - \sum_{(x, a^+, a^-)} \log \sigma(r(a^+|x) - r(a^-|x)).$$

For a given (x, a^+, a^-) , let

$$r^+ := r(a^+|x), \quad r^- := r(a^-|x),$$

the gradients with respect to r^+ and r^- are:

$$\begin{aligned}\frac{\partial \ell^{\text{RM}}}{\partial r^+} &= \frac{\partial \log(1 + e^{(r^- - r^+)})}{\partial r^+} = -\frac{e^{(r^- - r^+)}}{1 + e^{(r^- - r^+)}} = -\frac{1}{1 + e^{(r^+ - r^-)}}, \\ \frac{\partial \ell^{\text{RM}}}{\partial r^-} &= \frac{\partial \log(1 + e^{(r^- - r^+)})}{\partial r^-} = \frac{e^{(r^- - r^+)}}{1 + e^{(r^- - r^+)}} = \frac{1}{1 + e^{(r^+ - r^-)}}.\end{aligned}$$

This indicates that the gradients for the chosen and rejected responses are balanced and do not exhibit 3D-properties. In Section 5.2.1, we will further discuss the relationship between DPO and RLHF-PPO in real LLMs.

5 Experiments

In this section, we transition from theoretical analyses and toy model explorations to conducting real-world experiments with LLMs. These experiments are designed to validate the theoretical insights detailed in Section 3. The experimental setup is outlined in Section 5.1, with the main experimental results presented in Section 5.2 and a comparative analysis in Section 5.3.

5.1 Experimental Setup

Datasets. The alignment phase is commonly conducted to improve the model’s capabilities in mathematical reasoning and instruction following. Accordingly, we first validate our theory in the field of mathematics using the MATH dataset [14] as our primary experimental dataset⁴. Additionally, to evaluate the model’s out-of-distribution (OOD) generalization capabilities, we employed the SuperCLUE-Math benchmark [30]. To assess instruction-following abilities, we also created two in-house preference datasets focused on poem and slogan generation.

In practical applications, the commonly used datasets for the alignment stage cover various domains, and the sources of data can also be diverse. Thus, we further use a self-built general dataset consisting of approximately 400,000 preference samples, covering a diverse range of domains and the source of the data is also various, ranging from data generated by the model itself, data generated by GPT, and data from open-source datasets like HH-rlhf [6]. We designate this self-built dataset as "COMMON". The size of these datasets is detailed in Table 7 in the Appendix.

The LLMs of concern. We focus on Baichuan2-13B and Baichuan2-33B, an advanced bilingual (Chinese and English) LLM series. The 13B model is openly available [33], and the 33B model extends the 7B architecture with increased parameters.

5.2 The Effect of the Distribution of the Training Data.

Building on the theoretical insights presented in Section 3, we hypothesize that the performance of the vanilla DPO algorithm is influenced by the distribution characteristics of the training data, specifically whether they are on-policy or off-policy. For a detailed discussion on on-policy versus off-policy training, refer to Section A.1.

To generate on-policy responses, we used the model to be aligned to produce 8 candidates for each prompt in the MATH training set. Then, using GPT-4 [1], we selected the best and the worst responses from 8 candidates to form a preference pair. After applying filtering operations to exclude cases where all responses were uniformly good or bad, we compiled the MATH* dataset, which comprises 5826 training triplets x, a^+, a^- . We randomly select 2,000 samples from the original test set as the test set for MATH*. For off-policy chosen responses, we utilized the original solutions provided in the dataset. For the off-policy rejected responses, we employed responses generated by the Qwen1.5-7B model [5] for each prompt.

To validate the hypothesis, we implemented the settings described in the previous 4 scenarios shown in Figure 3. We used DPO to train the model under these scenarios respectively. After training, we test the performance of the model with the help of GPT-4. GPT-4 will assign scores ranging from 1-5 to each response, with responses scoring above 4 considered correct answers. The scoring criteria are

⁴Only the questions from the dataset were used to generate the preference dataset; details are provided in Section 5.2.

Table 1: The impact of training data being on-policy on the results. $\log \pi(a^+)$ and $\log \pi(a^-)$ denote the average log probability of each token of chosen response a^+ and rejected response a^- .

| | Baichuan2-13B | | Baichuan2-33B | |
|-------------------|-----------------|-----------------|-----------------|-----------------|
| | $\log \pi(a^+)$ | $\log \pi(a^-)$ | $\log \pi(a^+)$ | $\log \pi(a^-)$ |
| basemodel | -0.9181 | -0.9393 | -0.3603 | -0.3634 |
| DPO in Scenario 1 | -0.9681 | -0.9982 | -0.3629 | -0.3670 |
| basemodel | -1.6776 | -0.9238 | -1.4314 | -0.3525 |
| DPO in Scenario 2 | -1.6265 | -1.2293 | -1.2734 | -0.4254 |
| basemodel | -0.9461 | -1.7110 | -0.3460 | -1.1204 |
| DPO in Scenario 3 | -0.8786 | -1.8848 | -0.3439 | -1.4333 |
| basemodel | -1.7468 | -1.7110 | -1.2838 | -1.1451 |
| DPO in Scenario 4 | -1.6617 | -1.8265 | -1.2273 | -1.2234 |

Table 2: The performance tested on MATH* test set and SuperCLUE-Math.

| Setting | Baichuan2-13B | | Baichuan2-33B | |
|-------------------|----------------|----------------|----------------|----------------|
| | 5 points | 4&5 points | 5 points | 4&5 points |
| basemodel | 32.237% | 42.539 % | 44.485% | 53.229% |
| DPO in Scenario 1 | 37.132% | 47.082% | 47.465% | 54.759% |
| DPO in Scenario 2 | 32.860% | 43.445% | 44.216% | 51.409% |
| DPO in Scenario 3 | 28.323% | 41.576% | 44.473% | 53.924% |
| DPO in Scenario 4 | 26.833% | 37.685% | 46.618% | 54.648% |

detailed in Table 5. The average performance results on the MATH* and SuperCLUE-Math datasets are reported in Table 2. The specific experimental results for the two datasets are available in Tables 8 and 9. Additionally, we report the log probabilities before and after training in Table 1.

Among all 4 scenarios, Scenario 1 features both chosen and rejected responses as on-policy. This configuration ensures a more stable DPO training process, resulting in the best testing performance, as is shown in Table 2. According to Proposition 1, the critical factor determining the impact of 3D-properties is the decline rate of the likelihood of the rejected responses, $\log \pi(a^-)$. As is shown in Table 1, in comparison to other scenarios, Scenario 1 shows the slowest decline in likelihood, effectively mitigating the adverse effects of 3D-properties. This explains the superior performance of on-policy DPO in our tests.

We also plot the gradients during the training process of the DPO algorithm in scenario 1, which is shown in Figure 10 in the Appendix. This visualization corroborates the analysis presented in Section 3, demonstrating that the gradients for rejected responses increase more rapidly during training. Such an excessive decrease in the likelihood of generating rejected responses can ultimately contribute to model degradation. Additional analysis of the other scenarios is provided in Appendix D.

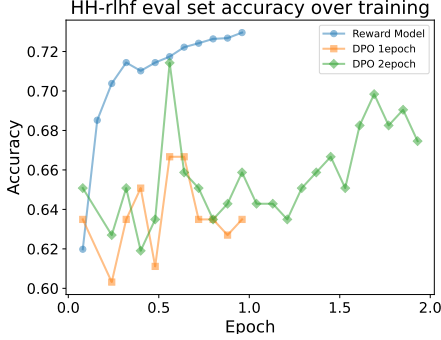
5.2.1 Suboptimality of DPO Algorithm Compared to RLHF-PPO Algorithm

In addition to mathematics datasets, we also tested the DPO algorithm and the commonly used RLHF-PPO algorithm on two self-built datasets regarding poem creation and slogan creation, respectively. These datasets have explicit scoring standards. For example, in the scenario of creating poems, the model needs to generate responses in different text and tone formats based on the given prompt. We set the metrics of a poem to the following five aspects: *Row Number*, *Words per Row*, *Rhythm*, *Tone Pattern* and *Title*, and set the metrics of a slogan to the following two aspects: *Word Count* and *Content*. For a detailed explanation of each metric, see Appendix C for detailed information. We use Baichuan2-33B to conduct the experiments and the results are shown in Table 3. As can be seen, the performance of DPO on both two datasets is worse than that of RLHF-PPO.

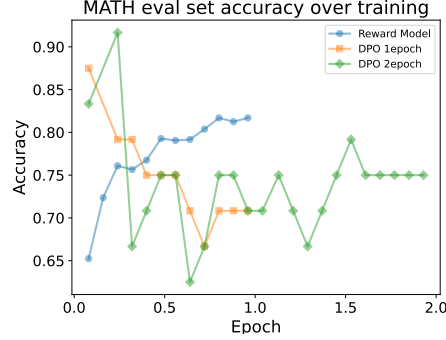
Following the regularization methods mentioned in Section 3.3, we fixed β_1 and gradually decreased β_2 . The results are shown in Figure 9 in the Appendix. As β_2 decreases, performance in poem

Table 3: The test result on self-built dataset Poem and Slogan. All the metrics are such that higher values are better.

| | Row Number | Poem | | | | Slogan | |
|----------|-------------|---------------|-------------|--------------|----------|-------------|-------------|
| | | Words per Row | Rhythm | Tone Pattern | Title | Word Count | Content |
| Base | 0.75 | 0.61 | 0.64 | 0.60 | 0.51 | 0.34 | 0.57 |
| RLHF-PPO | 0.91 | 0.79 | 0.87 | 0.82 | 1 | 0.47 | 0.78 |
| DPO | 0.93 | 0.75 | 0.83 | 0.75 | 0.78 | 0.45 | 0.70 |



(a) Accuracy of reward model and DPO on HH-rlhf eval set over the training process.



(b) Accuracy of reward model and DPO on MATH eval set over the training process.

Figure 4: Comparison between DPO and reward model training.

generation initially improves and subsequently declines. The initial improvement is intuitive and aligns with our expectations, as lowering β_2 slows the decrease of $\pi_\theta(a^-|x)$. However, we conjecture that an excessively low β_2 may cause DPO to perform like SFT on the chosen responses, thereby reducing its generalization capabilities. Additionally, we observe that other DPO variants like IPO and SLiC, despite having less severe 3D-properties effects, perform worse than DPO and PPO, which echoes Fact 2. One hypothesis is that their solution forms diverge significantly from the Bradley-Terry model, leading to a loss of generalization in preference learning. Both aspects demand further investigation. We provide a preliminary discussion in Appendix D and take them as parts of our future research.

5.3 Relative Instability of DPO Training Compared to Reward Model Training

Following Section 4, in this section, we conduct a direct comparison between DPO training and reward model (RM) training. Given that the objective function for DPO is derived from that used to train an RM, we simultaneously train an RM and conduct DPO training, allowing us to explicitly demonstrate the relative instability of DPO training.

We employ the Baichuan2-33B model for both DPO training and the initialization of the RM. The training preference dataset is our self-constructed COMMON dataset, and we test the two models on the widely used HH-rlhf dataset [6] and the MATH dataset [14]. We adopt accuracy as our metric, defined as the proportion of instances in which the model correctly identifies the chosen response as superior to the rejected one.

As is shown in Figure 4, the training process of the reward model is more stable, while the process of the DPO training fluctuates significantly. This observation aligns with the theoretical findings presented in Section 4, which state that 3D-properties do not exist in reward-based alignment methods. Furthermore, results from Figure 11 and Figure 12 show that the model trained using DPO is more likely to overfit the training data, reflecting a more aggressive optimization strategy.

6 Concluding Remarks and Limitations

In this study, we conducted a comprehensive theoretical analysis to elucidate why the widely used alignment algorithm DPO, does not perform as well as the RLHF-PPO algorithm. The principal challenge identified in DPO is summarized as 3D-properties. We substantiated our theoretical framework through experimental results obtained from both a toy model and real Large Language Models (LLMs) in practical applications, including mathematical reasoning and instruction following. Additionally, we assessed the effectiveness of specific regularization techniques. Furthermore, by contrasting DPO training with reward model training, we highlighted the inherent instability of DPO. We hope this work could offer research directions to narrow the gap between reward-free preference learning methods and reward-based ones. One limitation of this study is that we have not yet tested our theory on the recently proposed token-level reward DPO algorithm [37]. We plan to address this gap in future research.

References

- [1] Josh Achiam, Steven Adler, Sandhini Agarwal, Lama Ahmad, Ilge Akkaya, Florencia Leoni Aleman, Diogo Almeida, Janko Altenschmidt, Sam Altman, Shyamal Anadkat, et al. Gpt-4 technical report. *arXiv preprint arXiv:2303.08774*, 2023.
- [2] Afra Amini, Tim Vieira, and Ryan Cotterell. Direct preference optimization with an offset. *arXiv preprint arXiv:2402.10571*, 2024.
- [3] Anthropic. Introducing claude. <https://www.anthropic.com/claude>, 2024.
- [4] Mohammad Gheshlaghi Azar, Zhaohan Daniel Guo, Bilal Piot, Remi Munos, Mark Rowland, Michal Valko, and Daniele Calandriello. A general theoretical paradigm to understand learning from human preferences. In *International Conference on Artificial Intelligence and Statistics*, pages 4447–4455. PMLR, 2024.
- [5] Jinze Bai, Shuai Bai, Yunfei Chu, Zeyu Cui, Kai Dang, Xiaodong Deng, Yang Fan, Wenbin Ge, Yu Han, Fei Huang, et al. Qwen technical report. *arXiv preprint arXiv:2309.16609*, 2023.
- [6] Yuntao Bai, Andy Jones, Kamal Ndousse, Amanda Askell, Anna Chen, Nova DasSarma, Dawn Drain, Stanislav Fort, Deep Ganguli, Tom Henighan, et al. Training a helpful and harmless assistant with reinforcement learning from human feedback. *arXiv preprint arXiv:2204.05862*, 2022.
- [7] Ralph Allan Bradley and Milton E. Terry. Rank analysis of incomplete block designs: I. the method of paired comparisons. *Biometrika*, page 324, 1952.
- [8] Huayu Chen, Guande He, Hang Su, and Jun Zhu. Noise contrastive alignment of language models with explicit rewards. *arXiv preprint arXiv:2402.05369*, 2024.
- [9] Leshem Choshen, Lior Fox, Zohar Aizenbud, and Omri Abend. On the weaknesses of reinforcement learning for neural machine translation. *arXiv preprint arXiv:1907.01752*, 2019.
- [10] Aakanksha Chowdhery, Sharan Narang, Jacob Devlin, Maarten Bosma, Gaurav Mishra, Adam Roberts, Paul Barham, Hyung Won Chung, Charles Sutton, Sebastian Gehrmann, et al. Palm: Scaling language modeling with pathways. *Journal of Machine Learning Research*, 24(240):1–113, 2023.
- [11] Kawin Ethayarajh, Winnie Xu, Niklas Muennighoff, Dan Jurafsky, and Douwe Kiela. Kto: Model alignment as prospect theoretic optimization. *arXiv preprint arXiv:2402.01306*, 2024.
- [12] Duanyu Feng, Bowen Qin, Chen Huang, Zheng Zhang, and Wenqiang Lei. Towards analyzing and understanding the limitations of dpo: A theoretical perspective. *arXiv preprint arXiv:2404.04626*, 2024.
- [13] Shangmin Guo, Biao Zhang, Tianlin Liu, Tianqi Liu, Misha Khalman, Felipe Llinares, Alexandre Rame, Thomas Mesnard, Yao Zhao, Bilal Piot, et al. Direct language model alignment from online ai feedback. *arXiv preprint arXiv:2402.04792*, 2024.
- [14] Dan Hendrycks, Collin Burns, Saurav Kadavath, Akul Arora, Steven Basart, Eric Tang, Dawn Song, and Jacob Steinhardt. Measuring mathematical problem solving with the math dataset. *arXiv preprint arXiv:2103.03874*, 2021.

- [15] Zhenyu Hou, Yiin Niu, Zhengxiao Du, Xiaohan Zhang, Xiao Liu, Aohan Zeng, Qinkai Zheng, Minlie Huang, Hongning Wang, Jie Tang, et al. Chatglm-rlhf: Practices of aligning large language models with human feedback. *arXiv preprint arXiv:2404.00934*, 2024.
- [16] Albert Q Jiang, Alexandre Sablayrolles, Arthur Mensch, Chris Bamford, Devendra Singh Chaplot, Diego de las Casas, Florian Bressand, Gianna Lengyel, Guillaume Lample, Lucile Saulnier, et al. Mistral 7b. *arXiv preprint arXiv:2310.06825*, 2023.
- [17] Ziniu Li, Tian Xu, Yushun Zhang, Yang Yu, Ruoyu Sun, and Zhi-Quan Luo. Remax: A simple, effective, and efficient method for aligning large language models. *arXiv preprint arXiv:2310.10505*, 2023.
- [18] Tianqi Liu, Yao Zhao, Rishabh Joshi, Misha Khalman, Mohammad Saleh, Peter J Liu, and Jialu Liu. Statistical rejection sampling improves preference optimization. *arXiv preprint arXiv:2309.06657*, 2023.
- [19] Eric Mitchell. Online experimental results on dpo, 2023. https://wandb.ai/eric_anthony_mitchell/dpo-demos/runs/og8q3euz?nw=nwusereric_anthony_mitchell.
- [20] OpenAI. Introducing chatgpt, 2022. <https://openai.com/blog/chatgpt>, Last accessed on 2023-05-09.
- [21] Long Ouyang, Jeffrey Wu, Xu Jiang, Diogo Almeida, Carroll Wainwright, Pamela Mishkin, Chong Zhang, Sandhini Agarwal, Katarina Slama, Alex Ray, et al. Training language models to follow instructions with human feedback. *Advances in neural information processing systems*, 35:27730–27744, 2022.
- [22] Arka Pal, Deep Karkhanis, Samuel Dooley, Manley Roberts, Siddartha Naidu, and Colin White. Smaug: Fixing failure modes of preference optimisation with dpo-positive. *arXiv preprint arXiv:2402.13228*, 2024.
- [23] Rafael Rafailov, Archit Sharma, Eric Mitchell, Christopher D Manning, Stefano Ermon, and Chelsea Finn. Direct preference optimization: Your language model is secretly a reward model. *Advances in Neural Information Processing Systems*, 36, 2024.
- [24] John Schulman, Filip Wolski, Prafulla Dhariwal, Alec Radford, and Oleg Klimov. Proximal policy optimization algorithms. *arXiv preprint arXiv:1707.06347*, 2017.
- [25] Nisan Stiennon, Long Ouyang, Jeffrey Wu, Daniel Ziegler, Ryan Lowe, Chelsea Voss, Alec Radford, Dario Amodei, and Paul F Christiano. Learning to summarize with human feedback. *Advances in Neural Information Processing Systems*, 33:3008–3021, 2020.
- [26] Yunhao Tang, Daniel Zhaohan Guo, Zeyu Zheng, Daniele Calandriello, Yuan Cao, Eugene Tarassov, Rémi Munos, Bernardo Ávila Pires, Michal Valko, Yong Cheng, et al. Understanding the performance gap between online and offline alignment algorithms. *arXiv preprint arXiv:2405.08448*, 2024.
- [27] Gemini Team, Rohan Anil, Sebastian Borgeaud, Yonghui Wu, Jean-Baptiste Alayrac, Jiahui Yu, Radu Soricut, Johan Schalkwyk, Andrew M Dai, Anja Hauth, et al. Gemini: a family of highly capable multimodal models. *arXiv preprint arXiv:2312.11805*, 2023.
- [28] Hugo Touvron, Louis Martin, Kevin Stone, Peter Albert, Amjad Almahairi, Yasmine Babaei, Nikolay Bashlykov, Soumya Batra, Prajjwal Bhargava, Shruti Bhosale, et al. Llama 2: Open foundation and fine-tuned chat models. *arXiv preprint arXiv:2307.09288*, 2023.
- [29] Wei Xiong, Hanze Dong, Chenlu Ye, Ziqi Wang, Han Zhong, Heng Ji, Nan Jiang, and Tong Zhang. Iterative preference learning from human feedback: Bridging theory and practice for rlhf under kl-constraint. In *ICLR 2024 Workshop on Mathematical and Empirical Understanding of Foundation Models*, 2023.
- [30] Liang Xu, Hai Hu, Xuanwei Zhang, Lu Li, Chenjie Cao, Yudong Li, Yechen Xu, Kai Sun, Dian Yu, Cong Yu, et al. Clue: A chinese language understanding evaluation benchmark. *arXiv preprint arXiv:2004.05986*, 2020.
- [31] Shusheng Xu, Wei Fu, Jiaxuan Gao, Wenjie Ye, Weilin Liu, Zhiyu Mei, Guangju Wang, Chao Yu, and Yi Wu. Is dpo superior to ppo for llm alignment? a comprehensive study. *arXiv preprint arXiv:2404.10719*, 2024.
- [32] Yifan Xu, Xiao Liu, Xinghan Liu, Zhenyu Hou, Yueyan Li, Xiaohan Zhang, Zihan Wang, Aohan Zeng, Zhengxiao Du, Wenyi Zhao, et al. Chatglm-math: Improving math problem-solving in large language models with a self-critique pipeline. *arXiv preprint arXiv:2404.02893*, 2024.

- [33] Aiyuan Yang, Bin Xiao, Bingning Wang, Borong Zhang, Ce Bian, Chao Yin, Chenxu Lv, Da Pan, Dian Wang, Dong Yan, et al. Baichuan 2: Open large-scale language models. *arXiv preprint arXiv:2309.10305*, 2023.
- [34] Lifan Yuan, Ganqu Cui, Hanbin Wang, Ning Ding, Xingyao Wang, Jia Deng, Boji Shan, Huimin Chen, Ruobing Xie, Yankai Lin, et al. Advancing llm reasoning generalists with preference trees. *arXiv preprint arXiv:2404.02078*, 2024.
- [35] Susan Zhang, Stephen Roller, Naman Goyal, Mikel Artetxe, Moya Chen, Shuohui Chen, Christopher Dewan, Mona Diab, Xian Li, Xi Victoria Lin, et al. Opt: Open pre-trained transformer language models. *arXiv preprint arXiv:2205.01068*, 2022.
- [36] Yao Zhao, Rishabh Joshi, Tianqi Liu, Misha Khalman, Mohammad Saleh, and Peter J Liu. Slic-hf: Sequence likelihood calibration with human feedback. *arXiv preprint arXiv:2305.10425*, 2023.
- [37] Han Zhong, Guhao Feng, Wei Xiong, Li Zhao, Di He, Jiang Bian, and Liwei Wang. Dpo meets ppo: Reinforced token optimization for rlhf. *arXiv preprint arXiv:2404.18922*, 2024.
- [38] Daniel M Ziegler, Nisan Stiennon, Jeffrey Wu, Tom B Brown, Alec Radford, Dario Amodei, Paul Christiano, and Geoffrey Irving. Fine-tuning language models from human preferences. *arXiv preprint arXiv:1909.08593*, 2019.

A Detailed Background and Related Works

Large language models (LLMs) are profoundly transforming the way we work and live. Performing a three-stage process is the default practice for training LLMs: Pretraining, Supervised Fine-Tuning (SFT), and Reinforcement Learning from Human Feedback (RLHF). The roles of Pretraining and SFT are broadly understood: Pretraining encodes knowledge and SFT aligns question-answer formats. Relatively speaking, the understanding of RLHF is relatively insufficient. Specifically, Direct Preference Optimization (DPO) and its variants, as reward-model-free algorithms, have garnered significant attention due to their elegant mathematical form and relatively low resource requirements [23, 22, 13, 29]. However, it has also sparked considerable debate because of its unstable performance in practical applications [17, 31].

A.1 On-policy alignment vs. Off-policy alignment

The key inspiration for the DPO algorithm [23] is a closed-form solution to the RL step in RLHF, and thus an equivalent solution to the optimal policy for RLHF objective. The original DPO work is an off-policy learning algorithm for it relies on an extra preference dataset (Helpful-and-Harmless [6]), where the preference pairs are not generated by the policy LLM itself. On the other hand, there are a bunch of on-policy learning algorithms developed, where the preference responses are sampled from the policy model. [13] proposed the on-policy version of DPO. In on-policy DPO, all responses are sampled in a batch-wise way. A natural trade-off between them is the iterative DPO introduced by [29, 31]. The algorithm begins by initializing with an additional preference dataset, then iteratively trains a policy using DPO, collects response pairs through exploration policies, obtains preference signals from human or AI labelers, and updates the dataset with the newly labeled data.

A.2 Insights into DPO

Though the reward-free algorithms are favored due to their lower computational overhead, if they can achieve on-par performance with state-of-art reward-based methods such as RLHF-PPO sparked a lot of discussions. [18] proves that the absence of a reward model in DPO constrains its ability to sample preference pairs from the optimal policy. [31] show that DPO may have fundamental limitations that its optimal solution is a superset of the optimal solution of the PPO algorithm. This work also reports the empirical results that the performance of DPO is affected by the distribution shift between the model outputs and the preference dataset. [12] discusses the limitations of DPO from the perspective of gradient numerical stability, and conducted experiments to preliminarily verify it. However, they did not conduct experiments on real LLM and illustrate the correlation.

A.3 Other reward-free alignment algorithms

A major limitation of the DPO objective is its reliance on the Bradley-Terry model to convert pairwise preferences into point-wise rewards. To overcome this, [4] introduced Φ -preference optimization (Φ PO), where DPO is a special case of it that $\Phi(P) = \log \frac{P}{1-P}$. Identity-preference optimization (IPO) is a variant that replaces the Φ -function by an identity mapping function $\Phi(P) = P$.

Different from the DPO or IPO, the core idea of Sequence Likelihood Calibration (SLiC) [36] is to calibrate the likelihood of ranked sequences sampled from the policy being trained. The SLiC loss function can be decomposed into two parts: the rank function to guarantee that the difference between $\log \pi_{\theta}(a^+|x)$ and $\log \pi_{\theta}(a^-|x)$ is greater than δ under the current policy π_{θ} , and the cross-entropy regularizer that to encourage the model to stay close to the SFT model.

There are some other variants that tries to improve DPO, such as KTO [11], NCA [8], ODPO (DPO with an offset) [2]. KTO uses a Kahneman-Tversky model of human utility and proposes a method that directly maximizes the utility of generations instead of maximizing the log-likelihood of preferences. NCA leverages Noise Contrastive Estimation (NCE) to bridge the gap in handling reward datasets explicitly annotated with scalar evaluations. ODPO does not treat every preference pair equally during fine-tuning and requires the difference between the likelihood of the preferred and dispreferred response to be greater than an offset value.

B Theoretical Foundation

B.1 Fundamental Limitation in Vanilla DPO

Here we revisit the theoretical findings in Section 3.1. The loss function for vanilla DPO is given by

$$\ell^{\text{DPO}}(\theta) = \sum_{(x, a^+, a^-)} \log \left(1 + \left(\frac{\pi_0(a^+|x)}{\pi_0(a^-|x)} \frac{\pi_\theta(a^-|x)}{\pi_\theta(a^+|x)} \right)^\beta \right).$$

For a given (x, a^+, a^-) , let

$$\alpha := \left(\frac{\pi_0(a^+|x)}{\pi_0(a^-|x)} \right)^\beta, \quad \pi^+ := \pi(a^+|x), \quad \pi^- := \pi(a^-|x),$$

and

$$z = \frac{\pi_\theta(a^-|x)}{\pi_\theta(a^+|x)}.$$

Then we have

$$\begin{aligned} \frac{\partial \ell^{\text{DPO}}}{\partial \pi^+} &= \frac{\partial \log(1 + \alpha z^\beta)}{\partial z} \frac{\partial z}{\partial \pi^+} = \frac{\alpha \beta}{1 + \alpha z^\beta} z^{\beta-1} \frac{\partial z}{\partial \pi^+}, \\ \frac{\partial \ell^{\text{DPO}}}{\partial \pi^-} &= \frac{\partial \log(1 + \alpha z^\beta)}{\partial z} \frac{\partial z}{\partial \pi^-} = \frac{\alpha \beta}{1 + \alpha z^\beta} z^{\beta-1} \frac{\partial z}{\partial \pi^-}. \end{aligned}$$

Considering the case when $\pi^- \rightarrow 0$, we get $(\alpha \beta)/(1 + \alpha z^\beta) \rightarrow \alpha \beta$, thus,

$$\begin{aligned} \frac{\partial \ell^{\text{DPO}}}{\partial \pi^+} &\rightarrow -\alpha \beta (\pi^+)^{-\beta-1} (\pi^-)^\beta, \\ \frac{\partial \ell^{\text{DPO}}}{\partial \pi^-} &\rightarrow \alpha \beta (\pi^+)^{-\beta} (\pi^-)^{\beta-1}. \end{aligned}$$

As $\pi^- \rightarrow 0$, since $\beta < 1$, $\frac{\partial \ell^{\text{DPO}}}{\partial \pi^+}$ is proportional to $(\pi^-)^\beta$ and tends to 0, while $\frac{\partial \ell^{\text{DPO}}}{\partial \pi^-}$ is proportional to $(\pi^-)^{\beta-1}$ and tends to infinity. Therefore, in this case, the gradient for the rejected action becomes extremely large, while the gradient for the chosen action becomes very small.

Then we want to further explore the token-level gradient. Here, π^+ and π^- are the likelihood of the sequences. Let π_i^+ be the current selection probability of the i -th token for the chosen sequence, and let π_i^- be the current selection probability of the i -th token for the rejected sequence:

$$\begin{aligned} \pi^+ &= \prod_i \pi_i^+ = \pi_{-i}^+ \cdot \pi_i^+, \\ \pi^- &= \prod_i \pi_i^- = \pi_{-i}^- \cdot \pi_i^-. \end{aligned}$$

Here we have

$$\frac{\partial \pi}{\partial \pi_i} = \pi_{-i}.$$

Consider a softmax function:

$$s_i = \frac{e^{z_i}}{\sum_j e^{z_j}}.$$

The corresponding gradients are

$$\frac{\partial s_i}{\partial z_i} = s_i(1 - s_i), \quad \frac{\partial s_j}{\partial z_i} = -s_i s_j, \quad i \neq j.$$

Let

$$C(\pi^+, \pi^-) := \alpha \beta^+ (\pi^+)^{-\beta^+} (\pi^-)^{\beta^-}.$$

Therefore, considering the current selection probability π_i^+ of the i -th token for the chosen sequence, let the sampled token's index be c . The logit corresponding to this token c is denoted as $x_{i,c}^+$, then we have

$$\frac{\partial \ell^{\text{DPO}}}{\partial x_{i,c}^+} = \frac{\partial \ell^{\text{DPO}}}{\partial \pi^+} \frac{\partial \pi^+}{\partial \pi_i^+} \frac{\partial \pi_i^+}{\partial x_{i,c}^+} \rightarrow -C(\pi^+, \pi^-)(1 - x_{i,c}^+),$$

Let $c' \neq c$, we have

$$\frac{\partial \ell^{\text{DPO}'}}{\partial x_{i,c'}^+} = \frac{\partial \ell^{\text{DPO}'}}{\partial \pi^+} \frac{\partial \pi^+}{\partial \pi_i^+} \frac{\partial \pi_i^+}{\partial x_{i,c'}^+} \rightarrow C(\pi^+, \pi^-) x_{i,c'}^+.$$

Therefore, considering the current selection probability π_i^- of the i -th token for the rejected sequence, let the sampled token's index be c . The logit corresponding to this token c is denoted as $x_{i,c}^-$, then we have

$$\frac{\partial \ell^{\text{DPO}'}}{\partial x_{i,c}^-} = \frac{\partial \ell^{\text{DPO}'}}{\partial \pi^-} \frac{\partial \pi^-}{\partial \pi_i^-} \frac{\partial \pi_i^-}{\partial x_{i,c}^-} \rightarrow C(\pi^+, \pi^-) (1 - x_{i,c}^-),$$

Let $c' \neq c$, we have

$$\frac{\partial \ell^{\text{DPO}'}}{\partial x_{i,c'}^-} = \frac{\partial \ell^{\text{DPO}'}}{\partial \pi^-} \frac{\partial \pi^-}{\partial \pi_i^-} \frac{\partial \pi_i^-}{\partial x_{i,c'}^-} \rightarrow -C(\pi^+, \pi^-) x_{i,c'}^-.$$

We can see that the token-level gradients from the chosen response and the rejected response are at the same scale level. This reflects that DPO may not cause gradient numerical instability in the generation of a single token. However, if the impact of the algorithm on the state transition probability generated by autoregression is comprehensively considered, 3D-properties will still affect the performance of the algorithm.

B.2 Analysis on Regularization Techniques

In Section 3.3, we propose two straightforward regularization techniques. Here we provide theoretical analysis to see why they can mitigate 3D-properties.

B.2.1 Flexible β -DPO

The first technique employs variable values of β to control the rate at which the likelihood of rejected responses declines. Consider using different β^+ and β^- for the chosen and rejected responses:

$$\ell^{\text{flex-DPO}}(\theta) = - \sum_{(x, a^+, a^-)} \log \sigma \left[\beta^+ \log \frac{\pi_\theta(a^+|x)}{\pi_0(a^+|x)} - \beta^- \log \frac{\pi_\theta(a^-|x)}{\pi_0(a^-|x)} \right].$$

The loss function can be re-written by:

$$\ell^{\text{flex-DPO}}(\theta) = \sum_{(x, a^+, a^-)} \log \left(1 + \left(\frac{\pi_0(a^+|x)}{\pi_\theta(a^+|x)} \right)^{\beta^+} \left(\frac{\pi_\theta(a^-|x)}{\pi_0(a^-|x)} \right)^{\beta^-} \right).$$

For a given (x, a^+, a^-) , let

$$\alpha := \frac{\pi_0(a^+|x)^{\beta^+}}{\pi_0(a^-|x)^{\beta^-}}, \quad \pi^+ := \pi(a^+|x), \quad \pi^- := \pi(a^-|x),$$

and

$$z = \frac{\pi_\theta(a^-|x)^{\beta^-}}{\pi_\theta(a^+|x)^{\beta^+}}.$$

Then we have

$$\begin{aligned} \frac{\partial \ell^{\text{DPO}'}}{\partial \pi^+} &= \frac{\partial \log(1 + \alpha z)}{\partial z} \frac{\partial z}{\partial \pi^+} = \frac{\alpha}{1 + \alpha z} \frac{\partial z}{\partial \pi^+}, \\ \frac{\partial \ell^{\text{DPO}'}}{\partial \pi^-} &= \frac{\partial \log(1 + \alpha z)}{\partial z} \frac{\partial z}{\partial \pi^-} = \frac{\alpha}{1 + \alpha z} \frac{\partial z}{\partial \pi^-}. \end{aligned}$$

Considering the case when $\pi^- \rightarrow 0$, we get $\alpha/(1 + \alpha z) \rightarrow \alpha$, thus

$$\begin{aligned} \frac{\partial \ell^{\text{DPO}'}}{\partial \pi^+} &\rightarrow -\alpha \beta^+ (\pi^+)^{-\beta^+-1} (\pi^-)^{\beta^-}, \\ \frac{\partial \ell^{\text{DPO}'}}{\partial \pi^-} &\rightarrow \alpha \beta^- (\pi^+)^{-\beta^+} (\pi^-)^{\beta^--1}. \end{aligned}$$

Using different β^+ and β^- can only alleviate 3D-properties mentioned in Section 3.

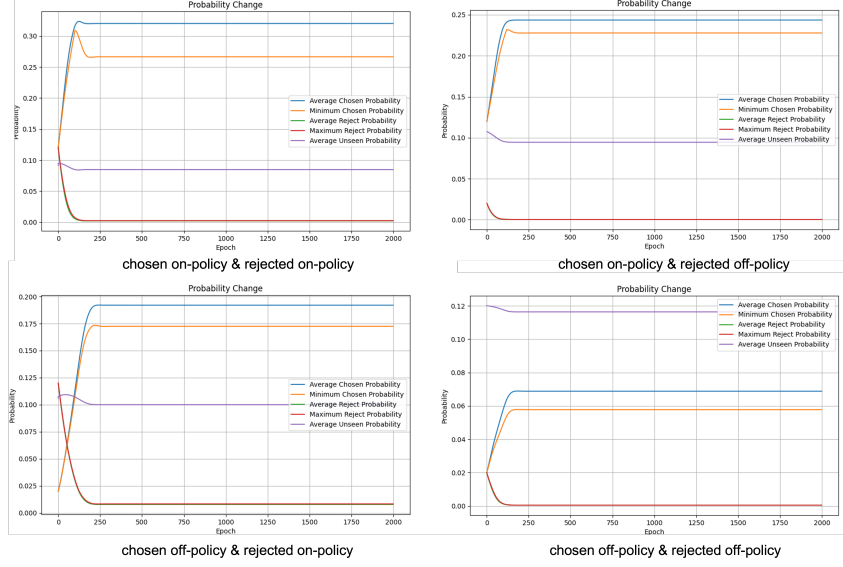


Figure 5: IPO performance on toy model.

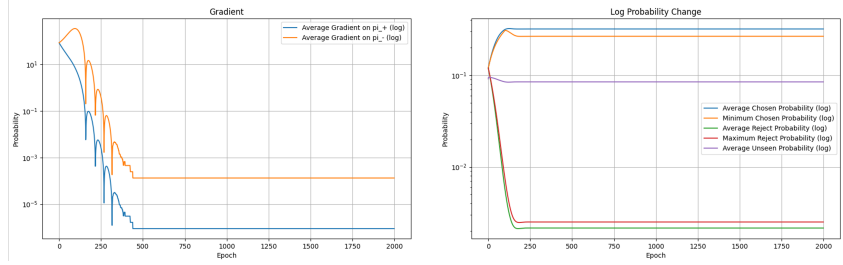


Figure 6: IPO Gradient and Log probability.

B.2.2 SFT Loss Regularization

The second technique involves augmenting the DPO loss with an SFT loss, a strategy that has been shown to significantly enhance the stability of DPO in previous studies. We can rewrite the loss function:

$$\ell^{\text{SFT-DPO}}(\theta) = - \sum_{(x, a^+, a^-)} \left\{ \log \sigma \left[\beta \log \frac{\pi_\theta(a^+|x)}{\pi_0(a^+|x)} - \beta \log \frac{\pi_\theta(a^-|x)}{\pi_0(a^-|x)} \right] - \gamma \log \pi_\theta(a^+|x) \right\} \quad (7)$$

Similarly, we have,

$$\frac{\partial \ell^{\text{SFT-DPO}}}{\partial \pi^+} = \frac{\partial \log(1 + \alpha z^\beta)}{\partial z} \frac{\partial z}{\partial \pi^+} = \frac{\alpha \beta}{1 + \alpha z^\beta} z^{\beta-1} \frac{\partial z}{\partial \pi^+} - \gamma \frac{1}{\pi^+},$$

$$\frac{\partial \ell^{\text{SFT-DPO}}}{\partial \pi^-} = \frac{\partial \log(1 + \alpha z^\beta)}{\partial z} \frac{\partial z}{\partial \pi^-} = \frac{\alpha \beta}{1 + \alpha z^\beta} z^{\beta-1} \frac{\partial z}{\partial \pi^-}.$$

As $\pi^- \rightarrow 0$, the gradient for the chosen action $\frac{\partial \ell^{\text{SFT-DPO}}}{\partial \pi^+} \rightarrow -\gamma \frac{1}{\pi^+} \neq 0$, which means the likelihood of chosen responses can be continually optimized.

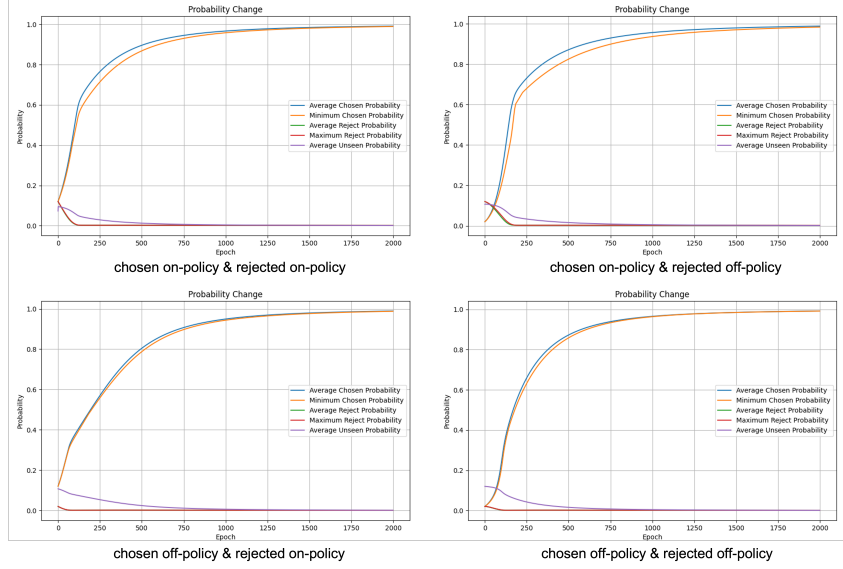


Figure 7: SLiC performance on toy model.

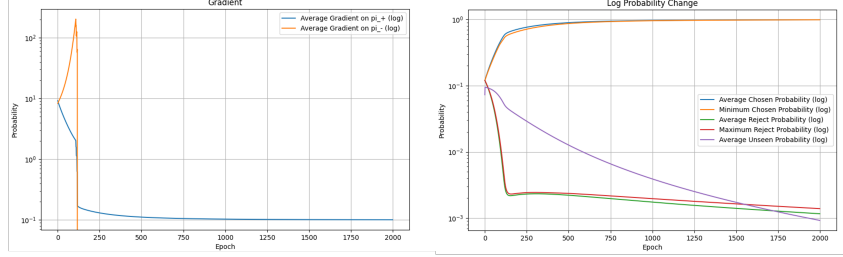


Figure 8: SLiC Gradient and Log probability.

B.3 Other invariants of DPO

B.3.1 Identity-preference Optimization (IPO)

In IPO, the loss function can be written by,

$$\ell^{\text{IPO}}(\theta) = \sum_{(x, a^+, a^-)} \left[\log \left[\frac{\pi_\theta(a^+|x)\pi_0(a^-|x)}{\pi_\theta(a^-|x)\pi_0(a^+|x)} \right] - \frac{1}{2\eta} \right]^2 \quad (8)$$

We directly give the gradients:

$$\frac{\partial \ell^{\text{IPO}}}{\partial \pi_\theta(a^-|x)} = -2 \left[\log \left[\frac{\pi_\theta(a^+|x)\pi_0(a^-|x)}{\pi_\theta(a^-|x)\pi_0(a^+|x)} \right] - \frac{1}{2\eta} \right] \cdot \frac{1}{\pi_\theta(a^-|x)} \quad (9)$$

$$\frac{\partial \ell^{\text{IPO}}}{\partial \pi_\theta(a^+|x)} = 2 \left[\log \left[\frac{\pi_\theta(a^+|x)\pi_0(a^-|x)}{\pi_\theta(a^-|x)\pi_0(a^+|x)} \right] - \frac{1}{2\eta} \right] \cdot \frac{1}{\pi_\theta(a^+|x)} \quad (10)$$

B.3.2 Sequence Likelihood Calibration (SLiC)

In SLiC, the loss function can be written by,

$$\ell^{\text{SLiC}}(\theta) = \sum_{x, a^+, a^-} \max [0, \delta - \log \pi_\theta(a^+|x) + \log \pi_\theta(a^-|x)] - \eta \cdot \log \pi_\theta(a^+|x) \quad (11)$$

if $\delta > \log \frac{\pi_\theta(a^+|x)}{\pi_\theta(a^-|x)}$:

Table 4: Data source of the responses in 4 scenarios.

| | chosen responses source | rejected responses source |
|------------|-------------------------|---------------------------|
| Scenario 1 | Baichuan2-33B | Baichuan2-33B |
| Scenario 2 | Solutions from dataset | Baichuan2-33B |
| Scenario 3 | Baichuan2-33B | Qwen-7B |
| Scenario 4 | Solutions from dataset | Qwen-7B |

Table 5: Evaluation criteria of the responses to the math questions.

| | |
|----------|--|
| 5 points | Full-score answer, requiring a correct response with the correct process, considering all possibilities, and being comprehensive. |
| 4 points | For complex questions, the answer is correct but lacks the process; for simple questions, the answer is correct but accompanied by a very redundant and verbose reasoning process. |
| 3 points | The answer is incorrect, but most of the process is correct, or the answer is correct, but there are obvious errors in the process. |
| 2 points | The answer is incorrect, and most of the process is incorrect. |
| 1 point | The answer and the entire process and thought process are incorrect, or the answer doesn't process to final result. |

$$\frac{\partial \ell^{\text{SLiC}}}{\partial \pi_{\theta}(a^+|x)} = -\frac{1+\eta}{\pi_{\theta}(a^+|x)}, \quad \frac{\partial \ell^{\text{SLiC}}}{\partial \pi_{\theta}(a^-|x)} = \frac{1}{\pi_{\theta}(a^-|x)} \quad (12)$$

else:

$$\frac{\partial \ell^{\text{SLiC}}}{\partial \pi_{\theta}(a^+|x)} = -\frac{\eta}{\pi_{\theta}(a^+|x)}, \quad \frac{\partial \ell^{\text{SLiC}}}{\partial \pi_{\theta}(a^-|x)} = 0 \quad (13)$$

These variants all alleviate the 3D-properties problem of DPO, so the results on mathematical reasoning are partly improved (see Table 10).

Remark 1. The invariants we tested do not perform well uniformly on all the tasks. For example, on instruction following tasks like poem generation, vanilla DPO outperforms SLiC and IPO. One hypothesis is their solution forms diverge significantly from the Bradley-Terry model, leading to a loss of generalization in preference learning.

C Dataset Description

Table 4 shows the data source for the LLM experiments in Section 5 in 4 scenarios. For example, in Scenario 1, the chosen and the rejected responses are both sampled from Baichuan2-33B and can be regarded as on-policy learning. In Scenario 4, the chosen responses are exactly the solutions given in the datasets while the rejected responses are sampled from another different LLM: Qwen-7B. In the experiments regarding Baichuan2-13B, we use the same data rather than re-sample the on-policy chosen responses. There are two reasons: 1. The 13B model is not as strong as the 33B model, therefore we can not sample enough high-quality responses as the chosen ones. 2. Models in the Baichuan2-series are all using the same dataset in Pretraining and SFT, therefore we can approximately think that their outputs are identically distributed. The log probability for the base model in Table 1 confirms this fact.

Table 5 describes the evaluation criteria of the responses to the math questions. A score of 5 means both the process and the result are correct, and a score of 4 or 5 means the answer is correct. We use these two indicators to evaluate the mathematical reasoning ability of the model. GPT-4 is used as the AI evaluator. We provide the evaluation prompt in our code in the supplementary material.

Table 6: Poem dataset test set.

| Poem type | Quatrain | Song Ci | Ancient Poetry | Metrical poetry | Modern poetry |
|----------------|----------|---------|----------------|-----------------|---------------|
| Test set Count | 138 | 518 | 93 | 173 | 85 |

Table 7: The statistic of used datasets.

| Setting | MATH* | SuperCLUE | Poem | Slogan | COMMON |
|-----------|-------|-----------|-------|--------|--------|
| train set | 5826 | - | 93269 | 13592 | 400000 |
| test set | 2000 | 1072 | 1000 | 1000 | - |

Table 6 shows the types of different poems in the poem dataset we used and their corresponding numbers in the test set. The language is all Chinese. Chinese poetry has strict format and rhyme requirements depending on the type. For example, for the quatrains, the row number must be 4, the number of words per row must be 5 or 7. The second and fourth sentences in the quatrain are required to rhyme, that is, the words at the end of the second and fourth sentences need to follow the prescribed tone. In this manner, we design a rule-based evaluation system to score each dimension of the generated answers. We selected the following characteristics as the basis for our evaluation:

- *Row Number*: For quatrain, the row number must be 4. For metrical poetry, the row number must be 8.
- *Words per Row*: For quatrain and metrical poetry, the number of words per row must be 8.
- *Rhythm*: Every type of poetry has a certain rhyme pattern requirement. Since it is a bit complicated to describe case by case, we put the requirements in the form of code in the supplementary material.
- *Tone Pattern*: For Song Ci, the tone pattern depends on the brand name.
- *Title*: Determined by the requirement in the prompt.

For the Slogan dataset, we evaluate the model’s performance based on whether it meets the word count requirements (*Word Count*) and the quality of the content (*Content*). We also provide the scoring and evaluation rule-based criteria in our code in the supplementary material.

Table 7 shows the amount of data in each dataset. MATH and SuperCLUE are open-source datasets, while Poem, Slogan, and COMMON are in-house self-built datasets. We provide part of the in-house datasets in the supplementary material to clarify the format and the content. SuperCLUE is only for cross-dataset testing, and COMMON is only used for the comparison between the reward model training and DPO training in Section 5.3.

D Experiments Details

D.1 Training Setting

In this section, we provide a detailed overview of our training settings. Following the implementation of [23], we use the Adam optimizer with the learning rate set to $5e-7$, and the default value for β was set to 0.1. We set the batch size to 80 and the number of gradient accumulation steps to 2. The training epoch was set to 1. In IPO training, we set η to be 0.1. In SLiC training, we set $\delta = 5$, $\eta = 0.1$. All experiments were conducted on a cluster consisting of 40 A100 GPUs.

D.2 Supplementary Experimental Results

Table 8 and Table 9 show the performance enhancement in MATH and SuperCLUE by vanilla DPO training respectively. It is easy to see that Scenario 1 where both the chosen responses and the rejected responses are on-policy performs best.

Figure 9 and Table 10 represent the additional results on DPO variants and regularization techniques. It can be seen that DPO variants can achieve on-par or better performance compared with vanilla

Table 8: Vanilla DPO: Baichuan2-13B accuracy on MATH* and SuperCLUE.

| | MATH* | | SuperCLUE | |
|------------|----------|------------|-----------|------------|
| | 5 points | 4&5 points | 5 points | 4&5 points |
| basemodel | 6.0% | 12.2% | 46.3% | 58.8% |
| Scenario 1 | 7.9% | 14.4% | 52.8% | 64.6% |
| Scenario 2 | 4.8% | 9.2% | 47.9% | 61.8% |
| Scenario 3 | 4.3% | 12.8% | 41.2% | 57.0% |
| Scenario 4 | 3.2% | 9.3% | 39.5% | 52.9% |

Table 9: Vanilla DPO: Baichuan2-33B accuracy on MATH* and SuperCLUE.

| | MATH* | | SuperCLUE | |
|------------|----------|------------|-----------|------------|
| | 5 points | 4&5 points | 5 points | 4&5 points |
| basemodel | 25.7% | 36.5% | 79.5% | 84.4% |
| Scenario 1 | 29.9% | 37.5% | 80.2% | 86.6% |
| Scenario 2 | 29.2% | 36.6% | 72.2% | 79.0% |
| Scenario 3 | 28.2% | 37.3% | 74.8% | 84.9% |
| Scenario 4 | 28.6% | 38.1% | 80.2% | 85.8% |

DPO. Figure 9 shows that as β_2 decreases, the performance in poem generation initially improves, reaches the peak point at around $\beta_2 = 0.08$, and subsequently declines. The initial improvement is intuitive. We conjecture that an excessively low β_2 may cause DPO to perform like SFT on the chosen responses, thereby reducing its generalization capabilities. For different tasks, the peak point of β_2 can be different. For example, in mathematical reasoning, we can set β_2 to be 0.01 and achieve better performance than vanilla DPO.

Figure 10 shows the change of the absolute value of gradient for the chosen and rejected responses ($\partial \ell^{\text{DPO}} / \partial \pi^+$ and $\partial \ell^{\text{DPO}} / \partial \pi^-$) during the training process of DPO on MATH. It can be seen that $|\partial \ell^{\text{DPO}} / \partial \pi^-| \gg |\partial \ell^{\text{DPO}} / \partial \pi^+|$, and the increasing rate of $\partial \ell^{\text{DPO}} / \partial \pi^-$ is much higher than that of $\partial \ell^{\text{DPO}} / \partial \pi^+$, which is align with Property 1.

Figure 11 and Figure 12 show the DPO convergence process with model trained on MATH and HH-rlhf respectively. In the second epoch, the accuracy growth of the model slows down sharply, which indicates that the model overfits the training data. The results further confirm that DPO is an aggressive optimization strategy compared to RLHF-PPO, and makes the impact of 3D-properties more prominent.

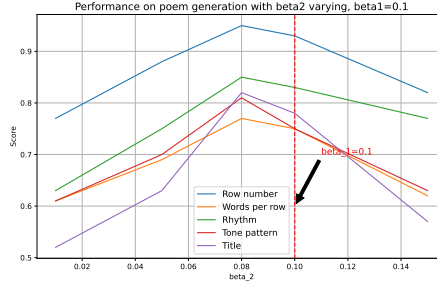
Figure 9: Performance on poem generation, β_2 varying with $\beta_1 = 0.1$.

Table 10: DPO and its variants/regularized version performance on mathematical reasoning. In Flex-DPO, $\beta_1 = 0.1$, $\beta_2 = 0.01$.

| | MATH* | | SuperCLUE | |
|-----------|--------------|--------------|--------------|--------------|
| | 5 points | 4&5 points | 5 points | 4&5 points |
| basemodel | 25.7% | 36.5% | 79.5% | 84.4% |
| DPO | 29.9% | 37.5% | 80.2% | 86.6% |
| Flex-DPO | 30.1% | 38.0% | 81.2% | 86.7% |
| IPO | 30.0% | 37.7% | 80.5% | 85.9% |
| SLiC | 29.3% | 38.7% | 79.7% | 84.5% |

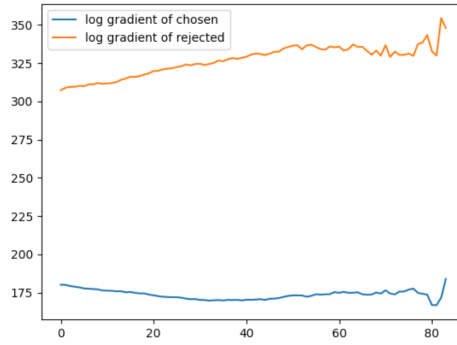
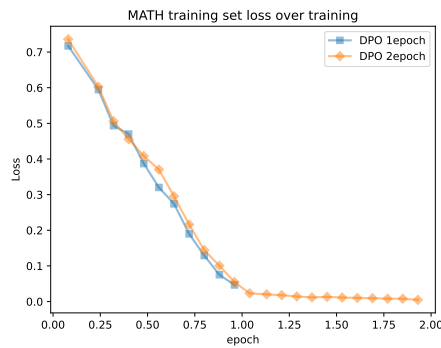
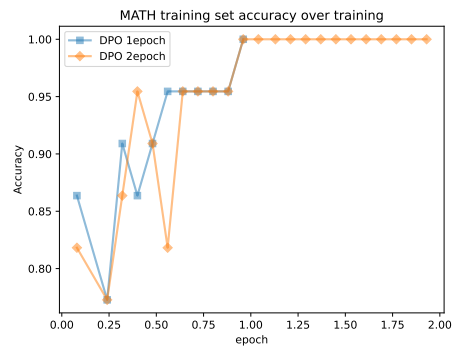


Figure 10: When training with on-policy data, the absolute value of the gradient for rejected responses increases, while the absolute value of the gradient for chosen responses remains almost unchanged.



(a) MATH train dataset loss.

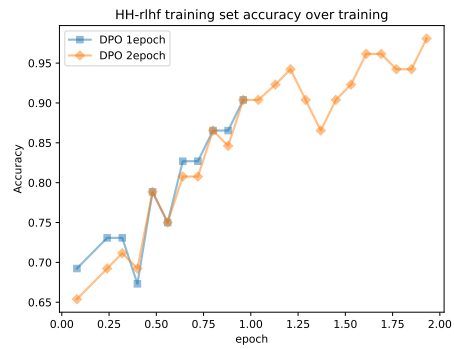


(b) MATH train dataset accuracy.

Figure 11: Comparison between DPO and reward model training on the training set of MATH. As can be seen, in the second epoch of DPO training, the loss is very small and the accuracy of distinguishing the chosen response from the rejected response is 100%, which indicates that the model overfits the training data.



(a) HH-rlhf train dataset loss.



(b) HH-rlhf train dataset accuracy.

Figure 12: Comparison between DPO and reward model training on the test set of HH-rlhf.